Supplematry information for

Low-loss and tunable localized mid-infrared plasmons in nanocrystals of highly-degenerate InN

Sadegh Askari[1,4*], Davide Mariotti[2], Jan Eric Stehr[3], Jan Benedikt[4], Julien Keraudy[1], Ulf Helmersson[1]

[1]Plasma & Coatings Physics Division, IFM-Material Physics, Linköping University, SE-581 83 Linköping, Sweden

[2]Engineering Research Institute (ERI), Ulster University, BT37 0QB, Northern Ireland, UK

[3]Department of Physics, Chemistry and Biology, Linköping University, 581 83 Linköping, Sweden

[4]Institute for Experimental and Applied Physics, Christian-Albrechts-Universität zu Kiel, Leibnizstraße 17, 24118 Kiel, Germany

Correspondence should be addressed S. Askari (askari@physik.uni-kiel.de)

S1: Pulsed plasma process for growth of nanocrystals

Plasma sputtering is a well-established method for growth of thin films. The method is based on eroding (or sputtering) the cathode (bulk material) using positively charged ions from a background inert gas. Ions are created by applying an electric field to the cathode in the presence of an inert gas (e.g. Ar) generating a plasma. Standard magnetron sputtering techniques have been previously employed for growth of sub-nanometer clusters or nanoparticles (named as *aggregation sources* [1-3]). However, adopting the technique to the tailored synthesis of nanocrystals (NCs) requires control over the growth phase of the NCs formation. The growth phase in *aggregation sources* is based on aggregation of nanoclusters through collisions at higher pressures provided in the aggregation chamber. Major problems are the lack of control over NCs properties such as size, possibility of agglomeration of the NCs, and issues with collecting NCs

(for instance due to the deposition on the reactor wall). Several approaches have been reported for size-selection of NCs emerged from the aggregation zone including the use of quadrupole mass filters [3] which can make the process complicated. Control over the growth stage, avoiding agglomeration and also control over the collection and assembly of NCs can promote the sputtering technique as a simple and reliable approach for producing NCs. The process presented here allows controlled growth of NCs of a broad range of functional materials (semiconductors, plasmonic metals etc.). In contrast to the aforementioned methods, our method is based on the nucleation and growth inside the plasma volume. As it will be shown here for InN NCs, the pulsed power technique provides a flexible process for controlled growth of NCs. In addition, charging inside the plasma volume results in collecting NCs without agglomeration and provides the opportunity for controlled collection of NCs. Several inherent advantages of this sputtering technique such as simplicity of using precursors in the bulk form, possibility of sputtering a wide range of materials and alloys can be exploited for growth of semiconducting NCs.

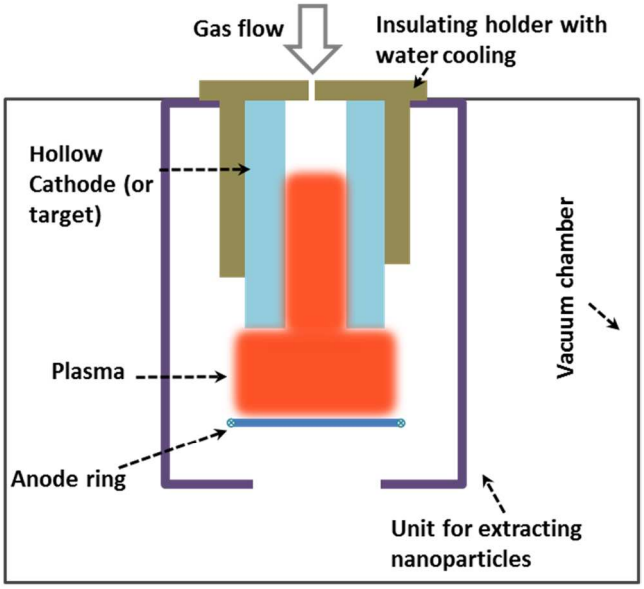

Figure S1: *Schematic of the experiment set-up for synthesis of nanocrystals using pulsed plasma process.*

The cathode is basically a hollow cylinder mounted inside a vacuum chamber with the base pressure 1.0×10^{-6} Torr. For the cathode, high purity (99.999% from Goodfellow) foil of indium with thickness 0.2 mm was used; the foil covers the surface of a cylindrical copper host with

length 55 mm and internal diameter of 7 mm. Argon gas flows through the hollow cathode and the plasma is maintained with applying pulsed electric field to the cathode. The argon plasma extends downstream of the cathode and fills the space between cathode and anode ring placed 35 mm from the cathode opening (figure S1). Applying short and intense electric pulses to the cathode produces highly ionized cloud [4] of the sputtered indium atoms that is blown out of the cathode exit and it expands longitudinally toward the anode. The highly dense cloud of ionized vapor provides an ideal medium for nucleation and formation of small (less than a nanometer) clusters of NCs through interaction of different species (metal ions, dissociated radical of the reactive gases, etc.). Larger nanoparticles are formed due to the agglomeration of these randomly charged small clusters; i.e. the small clusters in the plasma could be positive, negative or neutral and it facilitates their agglomeration. These nanoparticles with size of a few nanometers are negatively charged due to the high mobility of electron (relative to the ions) in plasma. As the nanoparticles are surrounded with a high density of positively charged ions (in the sputtered cloud), fast growth of nanoparticles is observed [4-5] due to the fast accretion of ions. The speed of the cloud out-puffed from the cathode is determined by the gas flow and also the intensity of the applied pulse. Typically it reaches to a few hundred meters per second at the cathode exit that moves the cloud away from the cathode around a few centimeter before the next pulse is applied (27 mm for f= 500 Hz [4]).

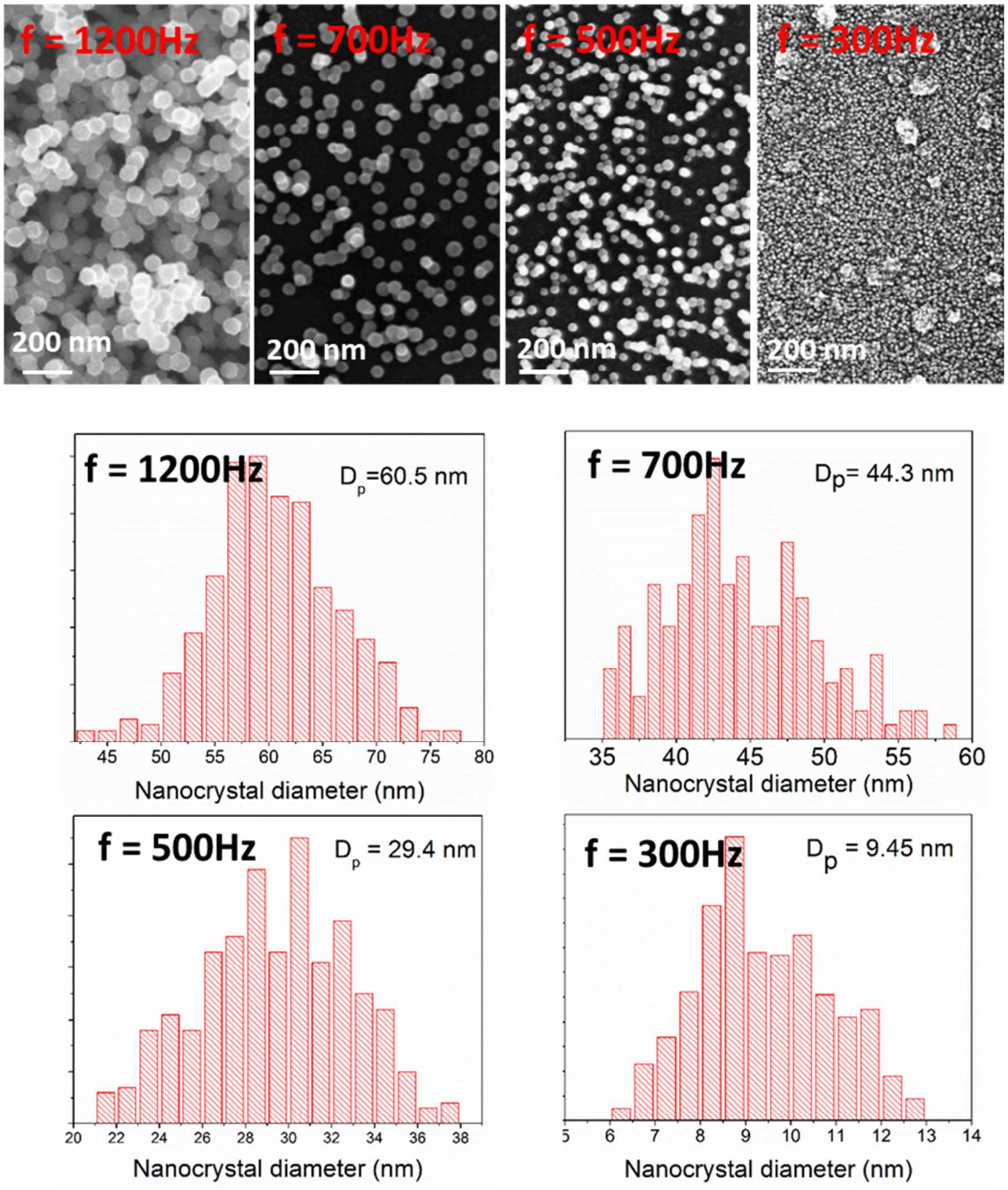

Figure S2: *scanning electron microscopy images and size distribution of InN nanocrystals prepared at four different applied electric pulse frequencies in the range 300-1200 Hz and the constant average applied power 20 W. D_p denotes the mean diameter.*

Fine tuning of the size was achieved by changing the pulse frequency. Figures S2 show the SEM images of NCs for four different pulse frequencies 300 Hz, 500 Hz, 700 Hz and 1200 Hz. The

average power was held constant at 20 W, which means that the peak current was lower for higher frequencies. The average NCs size is increased from 9.45 nm to 60.5 nm for this range of frequencies (figure S2). A typical nanoparticle is swept-over by ion pulses several times (depending on the pulse frequency) and thus the growth (for instance by ion accretion) is continued across the plasma volume.

Mass measurement of the collected NCs represents a deposition rate of the order of milligram per minute. For instance, at an applied average power of 20 W and a pulse frequency of 500 Hz, 5.4 mg powder is collected after 10 minutes of deposition. We should note however that the focus of this work was on the fundamental characteristics of the NCs and the role played by nitrogen deficiencies on the opto-electronic properties; for this reason the process is not optimized yet. For instance a drastic increase in mass production can be achieved by improving the collection efficiency and preventing NCs from being pumped out.

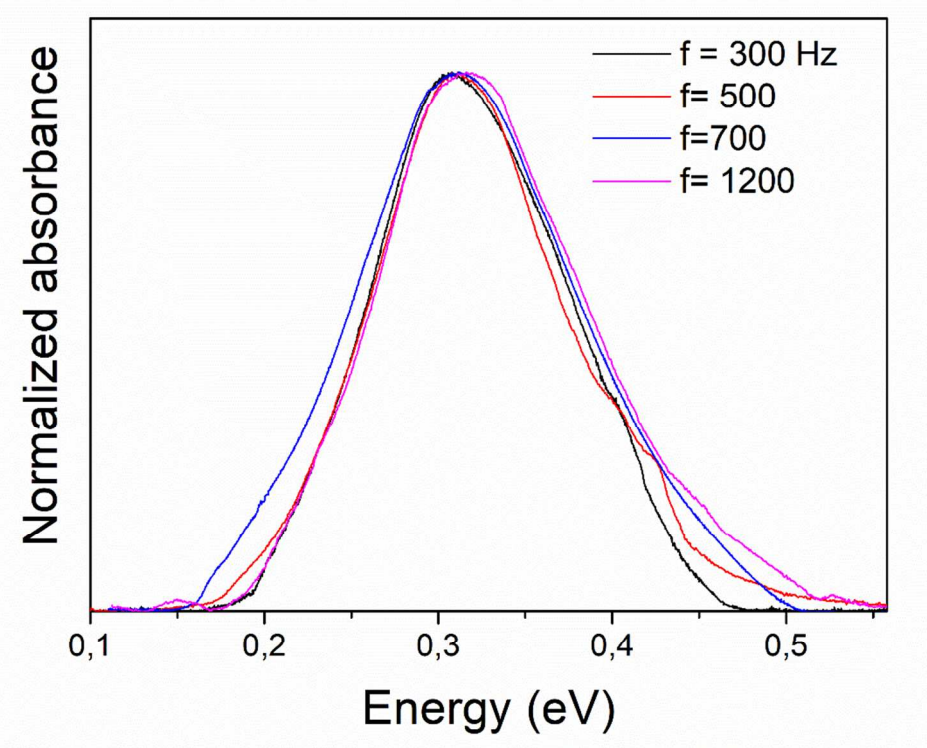

Figure S3*: The FTIR spectra of the InN nanocrystals for four different nanocrystal diameters.*

Figure S3 shows the FTIR spectra of these NCs with four different sizes. Its notable that the position of the IR absorption peak does not shift with NC diameter. Furthermore, EDX

measurement shows that the nitrogen deficiency remains unchanged in these samples. This corroborates the direct link of the nitrogen vacancy defects to the intense plasmonic absorption of NCs.

S2: Effective electron mass of degenerated InN

The effective electron mass in InN is linked to free electron density and a broad range of values from $0.039m_0$ for low electron density n_e= 1.8x10^{17}cm^{-3} to $0.25m_0$ for n_e=7x10^{20}cm^{-3} have been reported. The *k*-dependent effective electron mass is given by

$$m^*(k) = \frac{\hbar^2 k}{\frac{dE_C(k)}{dk}} \quad \text{(S1)}$$

where the $E_c(k)$ is given in eq.1 of the main manuscript; these take into account of the typical nonparabolicity of the conduction band [32]. The calculated electron effective mass as function of the free electron concentration for the E_g = 0.67eV and E_p=10 eV is plotted in figure S4.

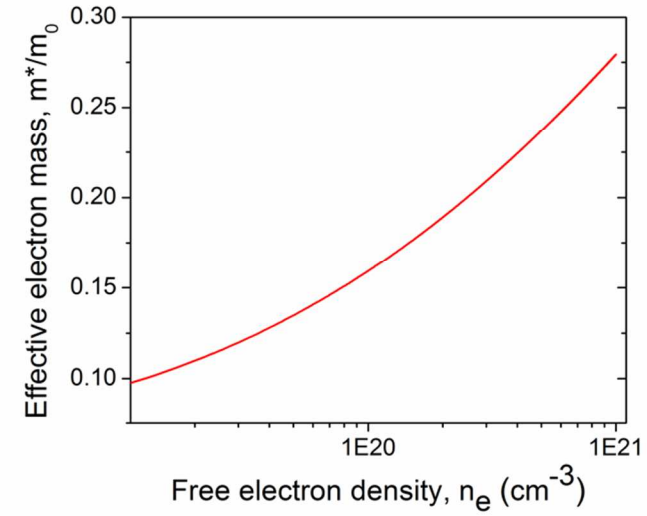

Figure S4: *InN effective electron mass as a function of free electron concentration calculated from the Kane's two band* ***k·p*** *model.*

S3: Free-electron density and electron mobility calculated from optical measurements

The free electron density can be obtained from its correlation with the plasmon resonance frequency (ω in eq. S6). This frequency can be calculated through using the expression for the dipole polarizability of a small nanocrystal with radius *r* much smaller than the wavelength of light given by

$$\alpha = 4\pi r^3 \frac{\varepsilon - \varepsilon_m}{\varepsilon + 2\varepsilon_m} \tag{S2}$$

where ε is the complex dielectric function of the plasmonic material and ε_m is the dielectric constant of the surrounding medium of the nanocrystal. The denominator of eq. S2 diminishes at the resonance condition when

$$\varepsilon_r = -2\varepsilon_m \tag{S3}$$

where ε_r is the real part of ε that is obtained from Drude model:

$$\varepsilon(\omega) = \varepsilon_r + i\varepsilon_i = \varepsilon_\infty - \frac{{\omega_p}^2}{\omega^2+\gamma^2} + i\frac{{\omega_p}^2\gamma}{\omega(\omega^2+\gamma^2)} \tag{S4}$$

where ε_∞ is the high frequency dielectric constant and is taken as 6.7 for InN, and γ is the damping parameter related to the scattering of electrons; it can be written as $\gamma = 1/\tau$ where τ is the average scattering time of electrons. In equation S4, ω_p is plasma frequency that is defined as

$${\omega_p}^2 = \frac{n_e \mathrm{e}^2}{\varepsilon_0 \mathrm{m}^*} \tag{S5}$$

Here n_e is the free electron density and m^* is the effective electron mass. The resonance frequency is obtained from eq. S3 where the real part of dielectric function is calculated from eq. S4

$$\omega_r = \sqrt{\frac{{\omega_p}^2}{\varepsilon_\infty + 2\varepsilon_m} - \gamma^2} \tag{S6}$$

The values for the electron densities are calculated from this equation as the resonance frequencies are known from the resonance absorption peaks (figure 2a). The electron mobility is related to the damping parameter throug $\mu = \frac{\mathrm{e}}{\gamma m^*}$.

S4: Optical band-gap calculated from the absorption

Optical band-gap displayed in figure 3b is calculated from the ultraviolet-visible absorption measurements.

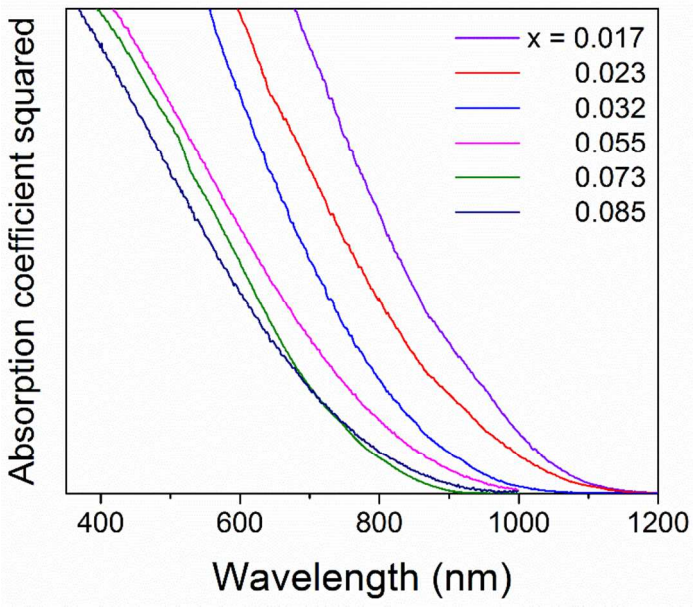

Figure S5: *squared absorption coefficient obtained from uv-visible absorption measurements for InN_{1-x} nanocrystals with varying nitrogen deficiency, 0.017<x<0.085.*

S5: Nitrogen vacancies donor and acceptor defects

The concentration of nitrogen vacancy defects including donor, acceptor and defects with neutral charge state can be estimated using density-functional theory calculations on the basis of favorable vacancies and formation energies. The calculations performed by Stampfl *et al.* [6] demonstrates the tendency to form neutral clusters in n-type InN. Negatively charged defects are also favored in clusters (e.g. with charge states -2, -3) while positively charged clusters generally occur with reduced positive charges. The details of the calculations including the binding energies and formation energies for clusters up to 6 vacancies with different charge states can be found in [6]. Here we calculate the concentration of the defects considering positively charged, neutral and negatively charged defects in the form of isolated and cluster vacancies.

The total number of nitrogen vacancies N_{total} is estimated from the nitrogen deficiency of the NCs that is varied in the range 0.54-2.70 x 10^{21} cm^{-3} corresponding to the chemical composition

of InN_{1-x} NCs with x = 0.017-0.085. The total number of vacancies is equal to the summation of vacancies

$$\sigma_D N_{D,q_D,\sigma_D} + \sigma_A N_{A,qA,\sigma_A} + \sigma_{neut} N_{\sigma_{neut}} = N_{total} \quad \text{(S7)}$$

Where the N_{D,q_D,σ_D}, N_{A,qA,σ_A} and $N_{\sigma_{neut}}$ are the concentration of donor, acceptor and neutral defects, respectively. σ_D, σ_A and σ_{neut} are the number of donor, acceptor and neutral vacancies in a single cluster. The balance of the electric charges is written as

$$q_D N_{D,q_D,\sigma_D} + q_A N_{A,qA,\sigma_A} = N_e \quad \text{(S8)}$$

where *Ne* is the concentration of the electron density. q_D and q_A are the electric charge state of the donor and acceptor defects, respectively where here we consider only charge states with the highest stability q_D = +1, and q_A = -2 (for σ_A = 3) and -3 (for σ_A = 4). The number of vacancy clusters with neutral charge state is expectedly higher than the negatively charged cluster and it gives

$$N_{\sigma_{neut}} \geq N_{A,qA,\sigma_A} \quad \text{(S9)}$$

The coupled eqs.S7 and S8 are solved with considering the lower limit for the neutral cluster concentration $N_{\sigma_{neut}} = N_{A,qA,\sigma_A}$. The values for the donor and acceptor concentration as a function of nitrogen deficiency is shown in figure 4a.

S6: Calculation of electron mobility limited by ionized defect scattering

Scattering by the ionized centers is the dominant factor limiting the mobility in degenerate InN. This mobility for a semiconductor with a narrow band-gap and non-parabolic conduction band is given by

$$\mu(k) = \frac{1}{q_D{}^2 N_{D,q_D,\sigma_D} + q_A{}^2 N_{A,qA,\sigma_A}} \frac{\varepsilon_s{}^2}{2\pi e^3 \hbar F_{imp}} k \left(\frac{dE}{dk}\right)^2 \quad \text{(S10)}$$

that is derived from the work by Zawadzki et *al.* on InSb [7]. In eq. S10, ε_s is the static dielectric constant and F_{imp} is a *k*-dependent function described in [7].

References

(1) Mantis nanoparticle deposition system. http://www.mantisdeposition.com/nanoparticlegenerators.html

(2) Palmer, R. E.; Pratontep, S.; Boyen, H. G. *Nature Materials* **2003**, 2, 443.

(3) Srivastava, S.; Thomas, J. P.; Rahman, Md. A.; Abd-Ellah, M.; Mohapatra, M.; Pradhan, D.; Heinig, N. F.; Leung, K. T. *ACS Nano* **2014**, 8, 11891.

(4) Hasan M. I.; Pilch, I.; D Soderstrom, Lundin, D.; Helmersson, U.; Brenning, N. *Plasma Sources Sci. Technol.* **2013**, 22, 035006.

(5) Pilch, I.; Söderström, D.; Hasan, M. I.; Helmersson, U., Brenning, N.; *App. Phys. Lett.* **2013**, 103, 193108.

(6) Duan, X. M.; Stampfl, C.; *Phys Rev B* **2008**, 77, 115207.

(7) Zawadzki, W.; Szymanka, W. *Phys. Stat. sol. (b)*, **1971**, 45, 415.